

Fig. 2. Structures of DNA adducts estimated from their detected *m/z* values indicated in Table 2. The structures of DMBA-DE-N⁶-dG and DMBA-DE-N²-dG were estimated by the adduction pattern of other PAH compounds.

approach to distinguish false-positive genotoxic compounds from MN-positive compounds. The reliability of this approach will be improved more if the sensitivity of LC/MS/MS equipment is increased and the adductome protocol is more sophisticated.

In summary, with the conditions in which the test compounds significantly increased the frequency of MN cells, only carcinogens (groups A and B) yielded adduct peaks as expected (Table 2 and Fig. 3). The advantages of this adductome approach are as follows: (1) multiple types of DNA adducts can be detected comprehen-

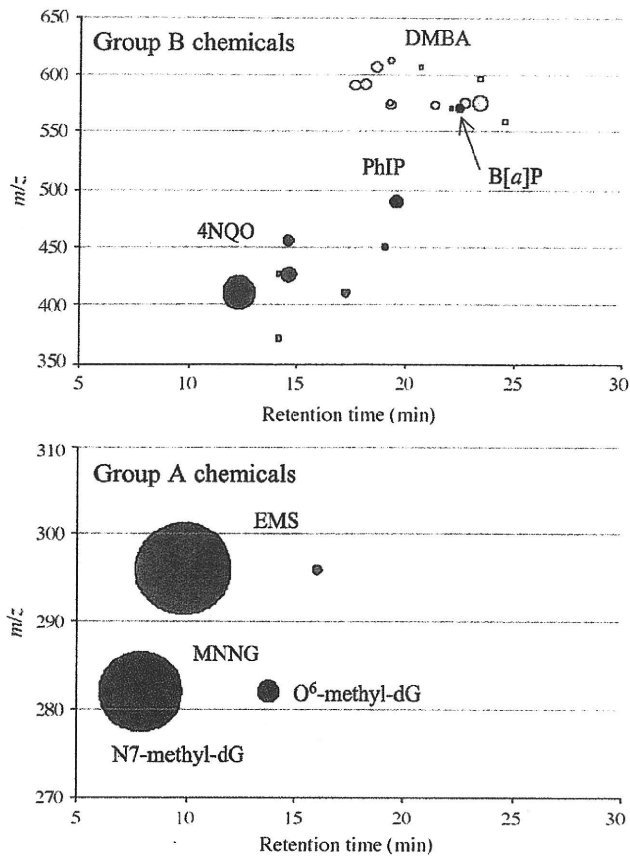


Fig. 3. DNA adductome maps of MN test positive carcinogens. CHL/IU cells were treated with Group A chemicals (carcinogens causing DNA alkylation) or Group B chemicals (carcinogens producing bulky DNA adducts), and the extracted DNA was digested by the MCN/SPD method (MNNG, EMS, B[a]P, DMBA) or nuclease P1 method (4-NQO and PhIP). The size of each bubble represents the "normalized peak area" shown in Table 2. Group A chemicals: EMS, pink; MNNG, brown. Group B chemicals: PhIP, blue; B[a]P, red; DMBA, yellow; 4-NQO, green. (For interpretation of the references to colour in this figure legend, the reader is referred to the web version of this article.)

sively, (2) the structures of the detected adducts can be identified from their m/z and their analytical standards, and (3) various experimental designs can be applied to both *in vitro* and *in vivo* samples. These experimental features resolve some limitations of the existing methods for analyzing DNA adduct formation.

This study is a pilot experiment to confirm the usefulness of the adductome approach to detect DNA adducts produced by the compounds showing positive results in the MN test with different MOA. This approach enables detection of various types of DNA adducts formed by typical carcinogens, and does not enable detection of any adducts for non-carcinogens. We conclude that the adductome approach would be applicable to assess the DNA-damaging capability of many types of *in vitro* MN test-positive compounds, and also be useful for understanding MOA of the test compounds.

Conflicts of interest

The authors have no conflicts of interest to declare.

Acknowledgements

This research was performed as a cooperative research project among three institutions, Mitsubishi Tanabe Pharma Corpora-

tion, Kyoto University, and Osaka Prefecture University, which was supported by a fund from Mitsubishi Tanabe Pharma Corporation.

Appendix A. Supplementary data

Supplementary data associated with this article can be found, in the online version, at doi:10.1016/j.mrgentox.2010.11.012.

References

- [1] D. Kirkland, M. Aardema, L. Henderson, L. Müller, Evaluation of the ability of a battery of 3 *in vitro* genotoxicity tests to discriminate rodent carcinogens and non-carcinogens. I. Sensitivity, specificity and relative predictivity, *Mutat. Res.* 584 (2005) 1–256.
- [2] G.M. Williams, J. Whysner, Epigenetic carcinogens: evaluation and risk assessment, *Exp. Toxicol. Pathol.* 48 (1996) 189–195.
- [3] D.H. Phillips, P.B. Farmer, F.A. Beland, R.G. Nath, M.C. Poirier, M.V. Reddy, K.W. Turteltaub, Methods of DNA adduct determination and their application to testing compounds for genotoxicity, *Environ. Mol. Mutagen.* 25 (2000) 222–233.
- [4] R.A. Kanaly, T. Hanaoka, H. Sugimura, H. Toda, S. Matsui, T. Matsuda, Development of the adductome approach to detect DNA damage in humans, *Antioxid. Redox Signal.* 8 (2006) 993–1001.
- [5] Y. Yang, D. Mikolic, S.M. Swanson, R.B. van Breeman, Quantitative determination of N⁷-methyldeoxyguanosine and O⁶-methyldeoxyguanosine in DNA by LC-UV-MS-MS, *Anal. Chem.* 74 (2002) 5376–5382.
- [6] D.T. Beranek, Distribution of methyl and ethyl adducts following alkylation with monofunctional alkylating agents, *Mutat. Res.* 231 (1990) 11–30.
- [7] P.D. Lowley, C.J. Thatcher, Methylation of deoxyribonucleic acid in cultured mammalian cells by N-methyl-N'-nitro-N-nitrosoguanidine, *Biochem. J.* 116 (1970) 693–707.
- [8] D. Lin, K.R. Kaderlik, R.J. Turesky, D.W. Miller, J.O. Lay Jr., F.F. Kadlubar, Identification of N-(deoxyguanosin-8-yl)-2-amino-1-methyl-6-phenylimidazo[4,5-b]pyridine as the major adduct formed by the food-borne carcinogen, 2-amino-1-methyl-6-phenylimidazo[4,5-b]pyridine, with DNA, *Chem. Res. Toxicol.* 5 (1992) 691–697.
- [9] Q. Ruan, H.H. Kim, H. Jiang, T.M. Penning, R.G. Harvey, I.A. Blair, Quantification of benzo[a]pyrene diol epoxide DNA-adducts by stable isotope dilution liquid chromatography/tandem mass spectrometry, *Rapid Commun. Mass Spectrom.* 20 (2006) 1369–1380.
- [10] K.W. Singletary, H.M. Parker, J.A. Milner, Identification and *in vivo* formation of ³²P-postlabeled rat mammary DMBA-DNA adducts, *Carcinogenesis* 11 (1990) 1959–1963.
- [11] S. Galiègue-Zoutina, B. Bailleul, M. Loucheux-Lefebvre, Adducts from *in vivo* aucton of the carcinogen 4-hydroxyaminoquinoline 1-oxide in rats and from *in vitro* reaction of 4-acetoxyaminoquinoline 1-oxide with DNA and polynucleotides, *Cancer Res.* 45 (1985) 520–525.
- [12] B. Bailleul, S. Galiègue, M. Loucheux-Lefebvre, Adducts from the Reaction of O, O'-diacetyl or o-acetyl derivatives of the carcinogen 4-hydroxyaminoquinoline 1-oxide with purine nucleosides, *Cancer Res.* 41 (1981) 4559–4565.
- [13] B. Bailleul, S. Galiègue-Zoutina, B. Perly, M. Loucheux-Lefebvre, Structural identification of the purine ring-opened form of N-(deoxyguanosine-8yl)-4-aminoquinoline 1-oxide, *Carcinogenesis* 6 (1985) 319–332.
- [14] S. Galiègue-Zoutina, B. Bailleul, Y. Ginot, B. Perly, P. Vigny, M. Loucheux-Lefebvre, N²-guanyl and N⁶-adenyl arylation of chicken erythrocyte DNA by the ultimate carcinogen of 4-nitroquinoline 1-oxide, *Cancer Res.* 46 (1986) 1858–1863.
- [15] Y. Arima, C. Nishigori, T. Takeuchi, S. Oka, K. Morimoto, A. Utani, Y. Miyachi, 4-nitroquinoline 1-oxide forms 8-hydroxydeoxyguanosine in human fibroblasts through reactive oxygen species, *Toxicol. Sci.* 91 (2006) 382–392.
- [16] T. Hofer, C. Badouard, E. Bajak, J. Ravanat, Å. Mattsson, I.A. Cotgreave, Hydrogen peroxide causes greater oxidation in cellular RNA than DNA, *Biol. Chem.* 386 (1995) 333–337.
- [17] H.S. Rosenkranz, F.K. Ennever, Evaluation of the genotoxicity of theobromine and caffeine, *Food Chem. Toxicol.* 25 (1987) 247–251.
- [18] W.U. Müller, T. Bauch, A. Wojcik, W. Böcker, C. Streffer, Comet assay studies indicate that caffeine-mediated increase in radiation risk of embryos is due to inhibition of DNA repair, *Mutagenesis* 11 (1996) 57–60.
- [19] K. Murakami, K. Ishida, K. Watanabe, R. Tsubouchi, M. Haneda, M. Yoshino, Prooxidant action of maltol: role of transition metals in the generation of reactive oxygen species and enhanced formation of 8-hydroxy-2'-deoxyguanosine formation in DNA, *Biomaterials* 19 (2006) 253–257.
- [20] S.M. Galloway, D.A. Deasy, C.L. Bean, A.R. Kravak, M.J. Armstrong, M.O. Bradley, Effects of high osmotic strength on chromosome aberrations, sister-chromatid exchanges and DNA strand breaks, and the relation to toxicity, *Mutat. Res.* 189 (1987) 15–25.

Efficient transfection method using deacylated polyethylenimine-coated magnetic nanoparticles

Daisuke Kami · Shogo Takeda · Hatsune Makino ·
Masashi Toyoda · Yoko Itakura · Satoshi Gojo ·
Shunei Kyo · Akihiro Umezawa · Masatoshi Watanabe

Received: 6 October 2010 / Accepted: 31 March 2011
© The Japanese Society for Artificial Organs 2011

Abstract Low efficiencies of nonviral gene vectors, such as transfection reagent, limit their utility in gene therapy. To overcome this disadvantage, we report on the preparation and properties of magnetic nanoparticles [diameter (d) = 121.32 ± 27.36 nm] positively charged by cationic polymer deacylated polyethylenimine (PEI max), which boosts gene delivery efficiency compare with polyethylenimine (PEI), and their use for the forced expression of plasmid delivery by application of a magnetic field. Magnetic nanoparticles were coated with PEI max, which enabled their electrostatic interaction with negatively charged molecules such as plasmid. We successfully

transfected $81.1 \pm 4.0\%$ of the cells using PEI max-coated magnetic nanoparticles (PEI max-nanoparticles). Along with their superior properties as a DNA delivery vehicle, PEI max-nanoparticles offer to deliver various DNA formulations in addition to traditional methods. Furthermore, efficiency of the gene transfer was not inhibited in the presence of serum in the cells. PEI max-nanoparticles may be a promising gene carrier that has high transfection efficiency as well as low cytotoxicity.

Keywords Deacylated polyethylenimine · Magnetic nanoparticle · Efficient nonviral transfection method

D. Kami
Innovative Integration between Medicine and Engineering Based on Information Communications Technology, Yokohama National University Global COE Program, Yokohama, Japan
e-mail: dkami@tmig.or.jp

S. Takeda · M. Watanabe (✉)
Laboratory for Medical Engineering, Division of Materials and Chemical Engineering, Yokohama National University, 79-1 Tokiwadai, Hodogaya-ku, Yokohama 240-8501, Japan
e-mail: mawata@ynu.ac.jp

D. Kami · H. Makino · M. Toyoda · A. Umezawa
Department of Reproductive Biology, National Institute for Child Health and Development, Tokyo, Japan

D. Kami · M. Toyoda (✉) · Y. Itakura · S. Gojo
Vascular Medicine, Research Team for Geriatric Medicine, Tokyo Metropolitan Institute of Gerontology, 35-2 Sakae-cho, Itabashi-ku, Tokyo 173-0015, Japan
e-mail: mtoyoda@tmig.or.jp

S. Gojo · S. Kyo
Division of Therapeutic Strategy for Heart Failure, Department of Cardio-Thoracic Surgery, The University of Tokyo, Tokyo, Japan

Introduction

Nanotechnologies that allow the nondisruptive introduction of carriers in vivo have wide potential for gene and therapeutic delivery systems [1–4]. Extremely small particles have been successfully introduced into living cells without any further modification to enhance endocytic internalization, such as for cationic help. The cells containing the internalized nanoparticles continued to thrive, indicating that the particles have no inhibitory effect on mitosis. Therefore, iron oxide magnetic nanoparticles have played an important role as magnetic resonance imaging contrast agents [5, 6], and cytotoxicity of this nanoparticle was none (or low) [7, 8]. Thereby, the functionalized iron oxide magnetic nanoparticles are expected to be useful as a new gene delivery tool [3].

Cationic polymer polyethylenimine (linear, MW 25,000) (PEI) is known as the transfection reagent in molecular biology [9], and the dispersant in nanotechnology [10]. PEI are configured to form the positively charged complex with DNA, which binds to anionic cell surface residues and

enter the cell via endocytosis [9, 11], keeping the dispersed state in the solution [10]. However, PEI containing residual *N*-acyl groups is a disadvantage for transfection efficiency. Also, the deacylated PEI (PEI max) for transfection reagent was reported, showing an increase in optimal transfection efficiency of 21-fold in comparison with PEI [12].

The transfection method using magnetic nanoparticles utilizes a magnetic force to deliver DNA into target cells. Therefore, the plasmid is first associated with magnetic nanoparticles. Then, the application of a magnetic force drives the plasmid–nanoparticle complexes toward and into the target cells, where the cargo is released (Fig. 1a) [13–16]. The magnetic nanoparticles are also coated with biological polymers, such as PEI, to allow plasmid loading (Fig. 1b). The binding of the negatively charged plasmid to the positively charged PEI max-coated magnetic nanoparticles (PEI max-nanoparticles) occurs relatively quickly. After complex formation, the loaded nanoparticles are incubated together with the target cells on a magnet plate. Owing to the magnetic force, the iron particles are rapidly drawn toward the surface of the cell membrane. Cellular uptake occurs by either endocytosis or pinocytosis [17]. Once delivered to the target cells, the plasmid is released into the cytoplasm [17, 18]. The magnetic nanoparticles accumulate in endosomes and/or vacuoles [18]. Over time, the nanoparticles are degraded and the iron enters normal iron metabolism [19]. An influence of magnetic nanoparticles on cellular functions has not been reported yet. However, in most cases, the increased iron concentration in culture media does not lead to cytotoxic effects [7].

In this study, we coated the transfection reagent, PEI max, on the surface of magnetic nanoparticles and applied a gene vector using PEI max-nanoparticles for a highly efficient transfection method. Our results indicate a high level of expression of the transfected gene in living cells using the plasmid-conjugated PEI max-nanoparticles.

Materials and methods

Materials

Magnetic nanoparticles (γ -Fe₂O₃, $d = 70$ nm) were purchased from CIK NanoTek. PEI max linear (MW 25,000) was purchased from Polysciences Inc. FuGENE HD was purchased from Roche Diagnostics. Deionized water was purchased from Gibco. Magnetic sheet (160 mT), and neodymium magnet (130 mT) was purchased from Magna Co. Ltd.

Preparation of the PEI max-nanoparticles

The magnetic nanoparticles (1.0 g) were dissolved in 30 ml of PEI max solution (1.6 mg PEI max/ml). The mixture was sonicated for 2 min (40 W) on ice, and 20 ml of deionized water was added (final concentration 1.0 mg PEI max/ml). The ferrofluid was centrifuged at 4,100 \times g for 5 min. The supernatant fluids were harvested and transferred into a fresh tube. This fluid was washed twice by deionized water and resolved into an equal volume of the PEI max solution (1.0 mg PEI max/ml). Magnetic

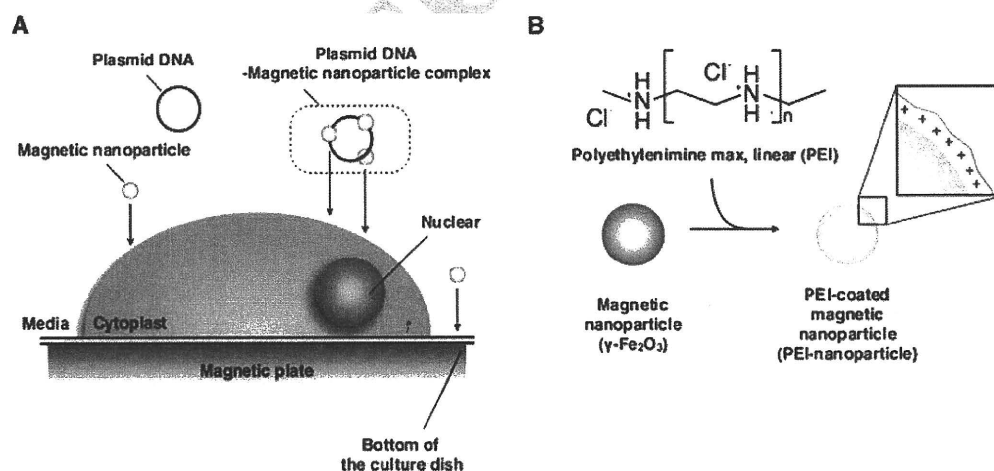


Fig. 1 Nanoparticle transfection method and cationic coating: **a** Plasmid-conjugated magnetic nanoparticles moved to the cell surface on the magnetic sheet upon application of magnetic force. Then, the magnetic force drove this complex toward and into the target cells. **b** Magnetic nanoparticles (γ -Fe₂O₃, $d = 70$ nm) (CIK NanoTek Inc.) were coated with deacylated polyethylenimine (PEI) max linear (MW

25,000) (Polysciences Inc.), known as a dispersive agent, and transfection reagents. The surface of the PEI max-nanoparticle was positively charged. Nanoparticles and plasmid formed complexes by ionic interaction of the negatively charged plasmid and the positively charged surface of the PEI max-nanoparticle

109	nanoparticles in this fluid were coated with PEI max and dispersed in PEI max solution or deionized water.	green fluorescent protein (EGFP), the modified pCAGGS expression vector [20], weight ratio PEI max:plasmid = 3:1 and incubated in the deionized water at final volume of 50 μ l at room temperature for 15 min. The complexes were added to the CL6 cells on a magnetic sheet various times (0, 0.5, 1, 4, and 24 h). Forty-eight hours after transfection, CL6 cells were evaluated; 1 mg/ml of PEI max solution was used as a positive control.	152 153 154 155 156 157 158 159
111	Measurement of PEI max-nanoparticle size and ζ -potential	Quantitative real-time reverse transcriptional (RT)-PCR	160
113	The size of the PEI max-nanoparticles was measured with a laser light-scattering method using a fiberoptics particle analyzer (FPAR-1000, Otsuka Electronics). The measurement was performed in triplicate, and median size and range of size distribution were obtained. The ζ -potential of the PEI max-nanoparticles was determined with electrophoretic light-scattering spectrophotometer (ELSZ-2, Otsuka Electronics).	Total RNAs from CL6 cells were extracted using ISOGEN (Nippon Gene). To perform quantitative real-time polymerase chain reaction (PCR) assay, total RNA (1 μ g) was reverse-transcribed using random hexamer and the Prime-Script RT reagent kit (TaKaRa). Quantitative real-time reverse transcriptional (RT)-PCR was performed on Line-Gen (BioFlux), using 100 ng of complementary DNA (cDNA) in 25- μ l reaction volumes with 10 nmol/l EGFP primer and 12.5 μ l of SYBR Premix Ex Taq (TaKaRa). PCR primers for the gene of EGFP and <i>Gapdh</i> were designed to amplify each cDNA using the sense primer (5'-CCGACCACATGAAGCAGCAC-3') and the reverse primer (5'-CTTCAGCTCGATGCGGTTTCAC-3') for the EGFP, and the sense primer (5'-TGCGACTTCAACAGCAACTC-3') and the reverse primer (5'-CTTGCTCAGTGTCTTGC TG-3') for the <i>Gapdh</i> . Calculations were automatically performed by fluorescent quantitative detection system software (BioFlux).	161 162 163 164 165 166 167 168 169 170 171 172 173 174 175 176 177 178
121	Charge characteristics of PEI max-nanoparticle	Nanoparticle cytotoxicity	179
122	PEI max-nanoparticle (100 μ g) and each weight of plasmid (2,000, 1,000, 750, 500, 375, 250, 188 ng) were mixed in deionized water or PEI max solution (1 mg/ml). Each solution were reacted for 1 h at room temperature.	Alamar Blue [21] was used to measure cell proliferation and metabolic activity as an oxidation-reduction indicator. After 48 h of PEI max or PEI max-nanoparticle exposure, 900 μ l of medium from each condition was transferred into a 24-well flat-bottomed plate. One hundred microliters of Alamar Blue (AbD Serotec) was added to each well, and the well plate was incubated for 3 h at 37°C. Fluorescence was measured at 570/600 nm in a Viento multispectrophotometer reader (Dainippon Pharmaceutical). The relative absorbance of CL6 cells without any treatment is regarded as 100% (it is indicated as a percent control in Fig. 4c).	180 181 182 183 184 185 186 187 188 189 190
126	Plasmid DNA was bound to PEI max-nanoparticles	Flow cytometric analysis	191
127	Plasmid DNA (5 μ g) was reacted with various weights of PEI max-nanoparticles (0–1.8 mg/tube) in deionized water for 15 min at room temperature. Then, the reaction mixtures were centrifuged at 12,000 \times g for 15 min and were formed in a sol-like precipitation in the lower layer. The concentration of DNA in the upper layer (hyaline layer) was determined by NanoDrop 1000 spectrophotometer (Thermo Scientific). The relative concentration of plasmid DNA treated without PEI max-nanoparticles was regarded as 100%.	To count the numbers of EGFP-positive cells using PEI max-nanoparticles (0.8 μ g/well in a six-well plate) on a magnetic sheet for 4 h (PEI max alone as a positive control), a Cytomics FC500 (Beckman Coulter Inc.) was used, and data were analyzed with FlowJo Ver.7 (Tree Star Inc.). Each sample was compared with negative control cells (without treatment).	192 193 194 195 196 197 198
137	Cell culture		
138	P19CL6 cells (CL6 cells) from a mouse embryonic carcinoma cell line were grown on 100-mm dishes (Becton-Dickinson) in alpha-minimum essential medium (MEM) (Nacalai Tesque) supplemented with 10% fetal bovine serum (FBS) (JRH Bioscience Inc.), penicillin, and streptomycin (Gibco), and were maintained in a 5% carbon dioxide (CO ₂) atmosphere at 37°C.		
145	Transfection procedure using PEI max-nanoparticles		
146	CL6 cells were seeded at 1×10^5 cells/well in six-well plates (Becton-Dickinson) 18 h before transfection. Immediately before transfection, cells were rinsed and supplemented with fresh culture medium (1 ml). The PEI max-nanoparticles (in 1 mg PEI max/ml solution) were mixed with 2.0 μ g of the plasmid [pCAGGS-enhanced		

199 Statistical analysis

200 Results, shown as the mean \pm standard error (SE), were
201 compared by analysis of variance (ANOVA) followed by
202 Scheffe test (<http://chiryo.phar.nagoya-cu.ac.jp/javastat/>
203 [JavaStat-j.htm](http://chiryo.phar.nagoya-cu.ac.jp/javastat/)), with $P < 0.05$ considered significant.

204 Results

205 Characterization of PEI max-nanoparticles

206 Magnetic nanoparticles were well coated with PEI max and
207 were highly dispersed in PEI max solution (1 mg/ml) or
208 deionized water. Secondary size of the PEI max-nanopar-
209 ticles was approximately 121.32 ± 27.36 nm (Fig. 2A).
210 To evaluate stability in PEI max solution (1 mg/ml) or
211 deionized water, we measured the ζ -potential of PEI max-
212 nanoparticles, which was $+45.53$ mV in PEI max solution
213 and $+30.05$ mV in deionized water. The PEI max-nano-
214 particles were aggregated by magnetic force (Fig. 2Ba) and
215 quickly redispersed by vortex (Fig. 2Bb). Time-lapse
216 photography (30 s/s) shows that magnetic nanoparticles
217 were gradually removed at the site of the neodymium
218 magnet (right side of the tube) for 2 h (magnetic nano-
219 particles for transfection: <http://www.youtube.com/watch?v=Hyjfc4moHK4>). These nanoparticles in PEI max solu-
220 tion were not aggregated without magnetic force. To avoid
221 aggregation of plasmid-attached PEI max-nanoparticle
222 caused by charge neutralization, it was necessary that their
223 weight ratio was approximately 1:400 (Fig. 2C). In gener-
224 al, 1–2 μ g of plasmid per well was mixed with the
225 transfection reagent such, as PEI max, and FuGENE HD
226 into six-well plates. However, too much (400–800 μ g of
227 nanoparticle per well) caused inhibition of transfection
228 (described later). To solve the problem, we decided to use
229 in 1 mg/ml of PEI max solution as a solvent. As a result,
230 each concentration of the plasmid did not aggregate with
231 PEI max-nanoparticle (Fig. 2Bb). To evaluate whether the
232 plasmid DNA was attached to PEI max-nanoparticles in
233 deionized water, we reacted PEI max-nanoparticles with
234 plasmid DNA for 15 min at room temperature. Measuring
235 the concentration of plasmid DNA in the upper layer
236 (hyaline layer), the weight of PEI max-nanoparticles was
237 reduced in a dependent manner (Fig. 2D).

239 Transfection efficiency using PEI max-nanoparticles
240 and magnetic sheet, and viability of the CL6 cells
241 treated with PEI max-nanoparticles

242 CL6 cells were transfected with pCAGGS-EGFP and PEI
243 max alone as a positive control (Fig. 3a) and pCAGGS-
244 EGFP and PEI max-nanoparticles (Fig. 3b) at 48 h after

transfection. Many EGFP-positive cells were observed
245 among CL6 cells transfected with PEI max-nanoparticles
246 compared with those transfected with PEI max. To
247 evaluate the optimum condition of transfection using PEI
248 max-nanoparticles, quantitative real-time RT-PCR was
249 performed at 48 h after transfection. The optimum con-
250 dition of transfection was a concentration of 0.8 μ g/well
251 (Fig. 4a) on a magnetic sheet for 4 h (Fig. 4b). *EGFP*
252 gene expression level was reduced under transfection of
253 excess magnetic nanoparticles (7.5 μ g/well) (Fig. 4a) and
254 prolonged time on the magnetic sheet (24 h) (Fig. 4b).
255 EGFP expression in CL6 cells transfected with PEI max-
256 nanoparticles was increased approximately two to four-
257 fold compared with those transfected with PEI max. The
258 viability of CL6 cells treated with PEI max-nanoparti-
259 cles, as measured by Alamar Blue assay, did not differ
260 between cells treated with/without PEI max alone
261 (Fig. 4c).

Number of EGFP-positive cells by flow cytometric
analysis

Forty-eight hours after transfection using PEI max alone or
265 PEI max-nanoparticles, we examined the number of EGFP-
266 positive cells (total 10,000 cells) by flow cytometric anal-
267 ysis. Compared with the negative control (untreated CL6
268 cells), $42.2 \pm 8.5\%$ of cells treated with PEI max alone
269 (Fig. 5a), $81.1 \pm 4.0\%$ of cells treated with 0.8 μ g of PEI
270 max-nanoparticles per well on the magnetic sheet for 4 h
271 (Fig. 5b), and $13.9 \pm 1.1\%$ of cells treated with FuGENE
272 HD (Fig. 5c) expressed EGFP. The number of EGFP-
273 positive cells was significantly increased (approximately
274 twofold) using PEI max-nanoparticles. 275

Discussion

In this study, to express target gene with high efficiency
277 and low cytotoxicity, we focused on PEI max and magnetic
278 nanoparticles (γ -Fe₂O₃). Many researchers have reported
279 various transfection methods using PEI and magnetic
280 nanoparticles, such as γ -Fe₂O₃, and superparamagnetic iron
281 oxide nanoparticle (used as magnetic resonance imaging
282 contrast agents) (Table 1). However, these methods had a
283 low transfection efficiency [14, 15], combined with virus
284 (adenovirus, or retrovirus) [15], and high cytotoxicity (low
285 cell viability) [13] and may therefore have little effec-
286 tiveness for clinical use. 287

The expression level of the *EGFP* gene was reduced
288 under transfection of excess magnetic nanoparticles
289 (7.5 μ g/well) (Fig. 4a). This result may indicate that a high
290 concentration of PEI max-nanoparticles formed the large
291 agglutinate complexes with plasmid DNAs [22, 23] 292

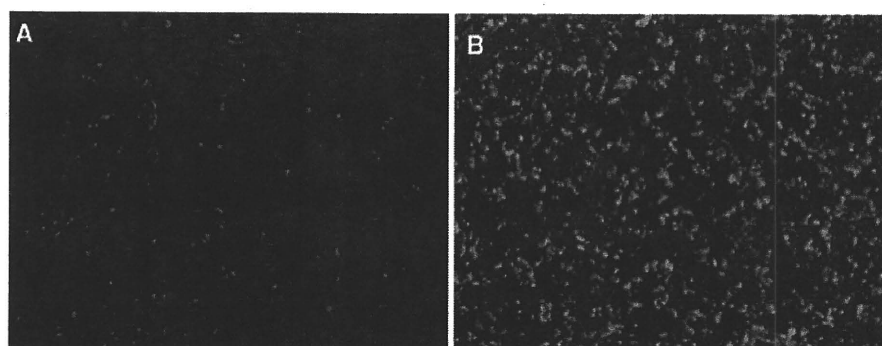


Fig. 3 Enhanced green fluorescent protein (EGFP) expression in CL6 cells using deacylated polyethylenimine (PEI max)-nanoparticle and magnetic field. Phase-contrast fluorescent micrograph of CL6 cells

were transfected with pCAGGS-EGFP and PEI max as a control (a) and PEI max-nanoparticles (b). The numbers of EGFP-positive cells were further increased by PEI max-nanoparticles

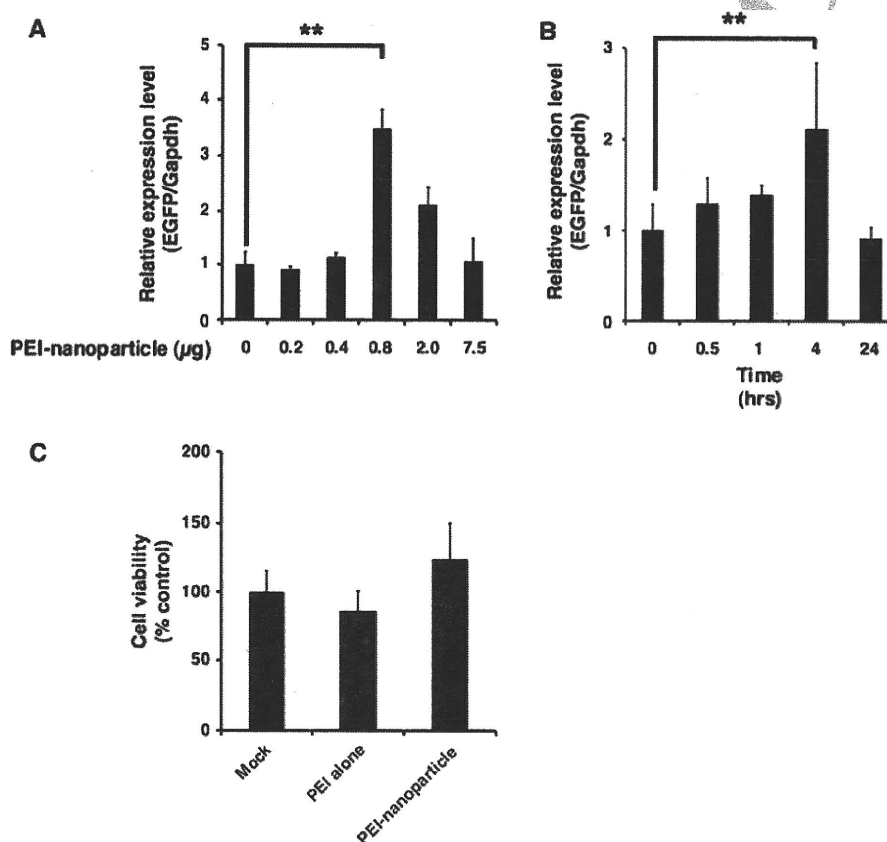


Fig. 4 Optimum condition for transfection of the deacylated polyethylenimine (PEI max)-nanoparticle. To optimize the transfection method, we examined PEI max-nanoparticles in terms of volume (a) and time (b) on the magnetic sheet. These results were evaluated by quantitative real-time reverse transcriptional polymerase chain reaction (RT-PCR). The expression level of the CL6 cells treated with PEI max alone is regarded as 1. The optimal conditions for transfection using PEI max-nanoparticles were when the CL6 cells were treated with 0.8 µg of PEI max-nanoparticles and 2.0 µg of pCAGGS-EGFP for 4 h on the magnetic sheet. The double asterisks

indicate a significant difference ($P < 0.05$). Cytotoxicities of PEI max and PEI max-nanoparticles were evaluated by Alamar Blue assay (c). After 48 h of PEI max or PEI max-nanoparticle exposure, there were no significant differences in cell viability between CL6 cells treated with PEI max and those with PEI max-nanoparticles. *Mock* the CL6 cells treated without any treatment as a negative control. *PEI max alone* the CL6 cells treated with PEI max. *PEI max-nanoparticles* the CL6 cells treated with PEI max-nanoparticles (0.8 µg) for 4 h on the magnetic sheet. The relative absorbance of untreated CL6 cells is regarded as 100%

Author Proof

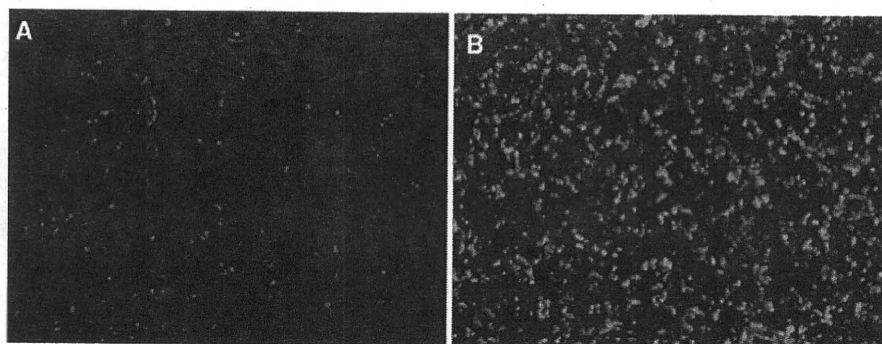


Fig. 3 Enhanced green fluorescent protein (EGFP) expression in CL6 cells using deacylated polyethylenimine (PEI max)-nanoparticle and magnetic field. Phase-contrast fluorescent micrograph of CL6 cells were transfected with pCAGGS-EGFP and PEI max as a control (a) and PEI max-nanoparticles (b). The numbers of EGFP-positive cells were further increased by PEI max-nanoparticles

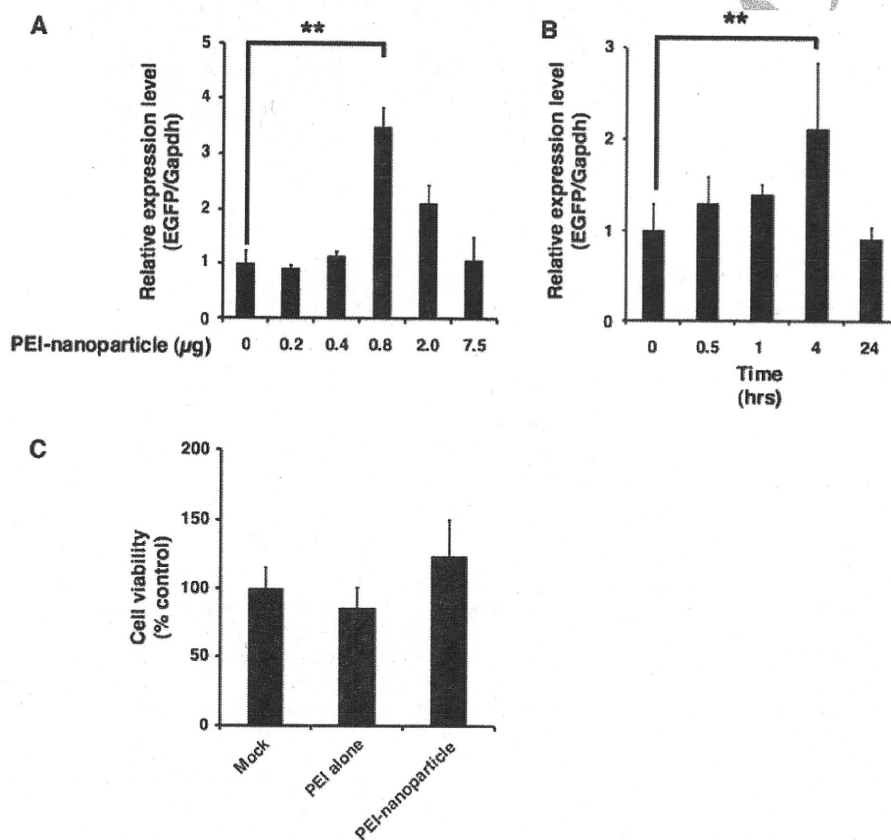


Fig. 4 Optimum condition for transfection of the deacylated polyethylenimine (PEI max)-nanoparticle. To optimize the transfection method, we examined PEI max-nanoparticles in terms of volume (a) and time (b) on the magnetic sheet. These results were evaluated by quantitative real-time reverse transcriptional polymerase chain reaction (RT-PCR). The expression level of the CL6 cells treated with PEI max alone is regarded as 1. The optimal conditions for transfection using PEI max-nanoparticles were when the CL6 cells were treated with 0.8 μg of PEI max-nanoparticles and 2.0 μg of pCAGGS-EGFP for 4 h on the magnetic sheet. The *double asterisks*

indicate a significant difference ($P < 0.05$). Cytotoxicities of PEI max and PEI max-nanoparticles were evaluated by Alamar Blue assay (c). After 48 h of PEI max or PEI max-nanoparticle exposure, there were no significant differences in cell viability between CL6 cells treated with PEI max and those with PEI max-nanoparticles. *Mock* the CL6 cells treated without any treatment as a negative control. *PEI max alone* the CL6 cells treated with PEI max. *PEI max-nanoparticles* the CL6 cells treated with PEI max-nanoparticles (0.8 μg) for 4 h on the magnetic sheet. The relative absorbance of untreated CL6 cells is regarded as 100%

Author Proof

Fig. 5 Transfection efficiency of the deacylated polyethylenimine (PEI max)-nanoparticle. Comparison of scattering properties of the untreated CL6 cells (mock, red dot) and with PEI max alone (a, blue dot, 42.2 ± 8.5%), PEI max-nanoparticles (b, blue dot, 81.1 ± 4.0%), or FuGENE HD (c, blue dot, 13.9 ± 1.1%) by flow cytometry

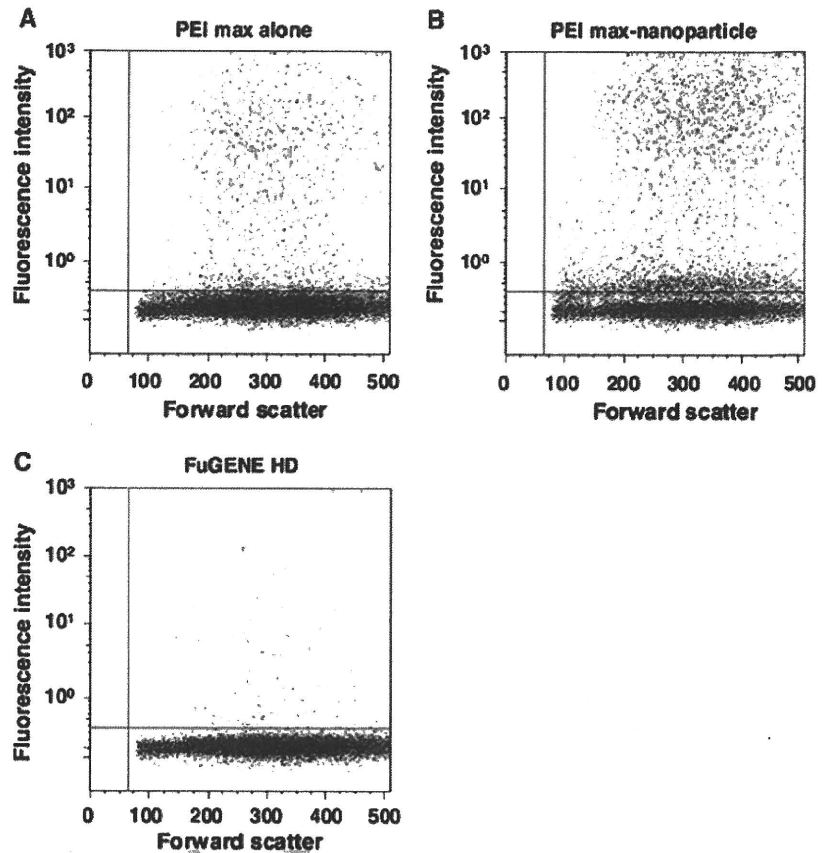


Table 1 Comparison of transfection methods using the polyethylenimine and magnetic nanoparticles

Author	Year	Vector	Component	Cell	Transfection efficiency	Cell viability (% of control)	References
Kami	-	Plasmid	PEI max (MW 25k), MNP (γ -Fe ₂ O ₃ , 70 nm), MF (0.2 T)	P19CL6	80% ^a	100	This paper
Zhang	2010	Plasmid	Branched PEI (MW 25k), SPION (30 nm), MF (1.2 T)	NIH3T3	64% ^a	100	[14]
		siRNA	Branched PEI (MW 25k), SPION (30 nm), MF (1.2 T)	NIH3T3	77% ^a	100	
Kievit	2009	Plasmid	PEI (MW 25k), SPION (200 nm)	C6	90% ^a	10	[13]
		Plasmid	PEI (MW 25k), Chitosan, SPION (200 nm)	C6	45% ^a	100	
		Plasmid	PolyMag (commercial magnification reagent), MF (1.2 T)	C6	32% ^a	66	
Scherer	2002	Plasmid	PEI (MW 800k), SPION (200 nm), MF (1 T)	NIH3T3	5-fold ^b	-	[15]
		Adenovirus	PEI (MW 800k), SPION (200 nm), MF (1 T)	K562	100-fold ^b	-	
		Retrovirus	PEI (MW 800k), SPION (200 nm), MF (1 T)	NIH3T3	20% ^a	-	

Transfection efficiency indicates optimal transfection condition

PEI polyethylenimine, PEI max deacylated PEI, MNP magnetic nanoparticle, SPION superparamagnetic iron oxide nanoparticle, MW molecular weight, MF magnetic force, T tesla

^a Flowcytometric analysis

^b Luciferase activity assay

315 efficiency. Furthermore, a major advantage of this method
 316 is its tolerability among cells. Other methods might be
 317 limited either by possible cytotoxic effects of the lipidic
 318 transfection reagent (lipofection) or simply by the directly
 319 applied force on the cells (electroporation). In contrast,
 methods such as lipofection offer only a certain probability
 of hits between cargo and cells because of the three-
 dimensional motion of cells and transfection aggregates in
 a liquid suspension. Normally, transfection was inhibited
 by serum using transfection reagent [25]. However, this

325 method can also be performed in the presence of serum,
326 which is a further benefit. Additionally, synergistic effects
327 on transfection efficiency can arise from the possible
328 combination of PEI max and nanoparticles. This technol-
329 ogy might be an alternative to the currently used viral and
330 nonviral vectors in gene therapy and gene transfer [26].

331 Our results suggest that PEI max-nanoparticles offer
332 the ability to deliver various DNA formulations in
333 addition to the traditional methods. Furthermore, gene
334 transfer efficiency was not inhibited in the presence of
335 serum in the cells. PEI max-nanoparticles may be a
336 promising gene carrier with high transfection efficiency
337 and low cytotoxicity.

338 **Acknowledgments** We express our sincere thanks to Koichiro
339 Nishino (Department of Reproductive Biology, National Institute for
340 Child Health and Development) for pCAGGS-EGFP. This study was
341 supported by a Grant-in-Aid for the Global COE Program, Science for
342 Future Molecular Systems, for SS and TO from the Ministry of
343 Education, Culture, Sports, Science and Technology, Japan (MEXT).

344 References

- 345 1. Kimura T, Iwai S, Moritan T, Nam K, Mutsuo S, Yoshizawa H,
346 Okada M, Furuzono T, Fujisato T, Kishida A. Preparation of
347 poly(vinyl alcohol)/DNA hydrogels via hydrogen bonds formed
348 on ultra-high pressurization and controlled release of DNA from
349 the hydrogels for gene delivery. *J Artif Organs*. 2007;10:104–8.
- 350 2. Moritake S, Taira S, Ichiyanagi Y, Morone N, Song SY, Hata-
351 naka T, Yuasa S, Setou M. Functionalized nano-magnetic parti-
352 cles for an in vivo delivery system. *J Nanosci Nanotechnol*.
353 2007;7:937–44.
- 354 3. Tomitaka A, Koshi T, Hatsugai S, Yamada T, Takemura Y. Magnetic
355 characterization of surface-coated magnetic nanoparticles for bio-
356 medical application. *J Magn Magn Mater*. 2010;323:1396–1403.
- 357 4. Yokoyama M. Drug targeting with nano-sized carrier systems.
358 *J Artif Organs*. 2005;8:77–84.
- 359 5. Lauterbur PC, et al. Image formation by induced local interac-
360 tions. Examples employing nuclear magnetic resonance. *Clin*
361 *Orthop Relat Res*. 1973;1989:3–6.
- 362 6. Nakamura H, Ito N, Kotake F, Mizokami Y, Matsuoka T. Tumor-
363 detecting capacity and clinical usefulness of SPIO-MRI in patients
364 with hepatocellular carcinoma. *J Gastroenterol*. 2000;35:849–55.
- 365 7. Karlsson HL, Cronholm P, Gustafsson J, Moller L. Copper oxide
366 nanoparticles are highly toxic: a comparison between metal oxide
367 nanoparticles and carbon nanotubes. *Chem Res Toxicol*.
368 2008;21:1726–32.
- 369 8. Karlsson HL, Gustafsson J, Cronholm P, Moller L. Size-depend-
370 ent toxicity of metal oxide particles—a comparison between
371 nano- and micrometer size. *Toxicol Lett*. 2009;188:112–8.
- 372 9. Boussif O, Lezoualc'h F, Zanta MA, Mergny MD, Scherman D,
373 Demeneix B, Behr JP. A versatile vector for gene and oligonu-
374 cleotide transfer into cells in culture and in vivo: polyethyleni-
375 mine. *Proc Natl Acad Sci USA*. 1995;92:7297–301.
- 376 10. Wang J, Gao L. Adsorption of polyethylenimine on nanosized
377 zirconia particles in aqueous suspensions. *J Colloid Interface Sci*.
378 1999;216:436–9.

- 379 11. Vancha AR, Govindaraju S, Parsa KV, Jasti M, Gonzalez-Garcia
380 M, Ballester RP. Use of polyethyleneimine polymer in cell
381 culture as attachment factor and lipofection enhancer. *BMC*
382 *Biotechnol*. 2004;4:23.
- 383 12. Thomas M, Lu JJ, Ge Q, Zhang C, Chen J, Klibanov AM. Full
384 deacylation of polyethylenimine dramatically boosts its gene
385 delivery efficiency and specificity to mouse lung. *Proc Natl Acad*
386 *Sci USA*. 2005;102:5679–84.
- 387 13. Kievit FM, Veiseh O, Bhattarai N, Fang C, Gunn JW, Lee D,
388 Ellenbogen RG, Olson JM, Zhang M. PEI-PEG-chitosan
389 copolymer coated iron oxide nanoparticles for safe gene delivery:
390 synthesis, complexation, and transfection. *Adv Funct Mater*.
391 2009;19:2244–51.
- 392 14. Zhang H, Lee MY, Hogg MG, Dordick JS, Sharfstein ST. Gene
393 delivery in three-dimensional cell cultures by superparamagnetic
394 nanoparticles. *ACS Nano*. 2010;4:4733–43.
- 395 15. Scherer F, Anton M, Schillinger U, Henke J, Bergemann C,
396 Kruger A, Gansbacher B, Plank C. Magnetofection: enhancing
397 and targeting gene delivery by magnetic force in vitro and in
398 vivo. *Gene Ther*. 2002;9:102–9.
- 399 16. Bertram J. MATra—magnet assisted transfection: combining nano-
400 technology and magnetic forces to improve intracellular delivery of
401 nucleic acids. *Curr Pharm Biotechnol*. 2006;7:277–85.
- 402 17. Arsianti M, Lim M, Marquis CP, Amal R. Polyethylenimine
403 based magnetic iron-oxide vector: the effect of vector component
404 assembly on cellular entry mechanism, intracellular localization,
405 and cellular viability. *Biomacromolecules*. 2010;11:2521–31.
- 406 18. Georgieva JV, Kalicharan D, Couraud PO, Romero IA, Weksler
407 B, Hoekstra D, Zuhom IS. Surface characteristics of nanoparti-
408 cles determine their intracellular fate in and processing by human
409 blood-brain barrier endothelial cells in vitro. *Mol Ther*.
410 2011;19:318–25.
- 411 19. Longmire M, Choyke PL, Kobayashi H. Clearance properties of
412 nano-sized particles and molecules as imaging agents: consider-
413 ations and caveats. *Nanomedicine (Lond)*. 2008;3:703–17.
- 414 20. Niwa H, Yamamura K, Miyazaki J. Efficient selection for high-
415 expression transfectants with a novel eukaryotic vector. *Gene*.
416 1991;108:193–9.
- 417 21. Nakayama GR, Caton MC, Nova MP, Parandoosh Z. Assessment
418 of the Alamar blue assay for cellular growth and viability in vitro.
419 *J Immunol Methods*. 1997;204:205–8.
- 420 22. Namgung R, Singha K, Yu MK, Jon S, Kim YS, Ahn Y, Park IK,
421 Kim WJ. Hybrid superparamagnetic iron oxide nanoparticle-
422 branched polyethylenimine magnetoplexes for gene transfection
423 of vascular endothelial cells. *Biomaterials*. 2010;31:4204–13.
- 424 23. Song HP, Yang JY, Lo SL, Wang Y, Fan WM, Tang XS, Xue JM,
425 Wang S. Gene transfer using self-assembled ternary complexes of
426 cationic magnetic nanoparticles, plasmid DNA and cell-pene-
427 trating Tat peptide. *Biomaterials*. 2010;31:769–78.
- 428 24. Coonrod A, Li FQ, Horwitz M. On the mechanism of DNA
429 transfection: efficient gene transfer without viruses. *Gene Ther*.
430 1997;4:1313–21.
- 431 25. Puro BW, Sundaresan TK, Burdick MJ, Kefas BA, Comeau
432 LD, Hawkinson MP, Su Q, Kotliarov Y, Lee J, Zhang W, Fine
433 HA. Notch-1 regulates transcription of the epidermal growth
434 factor receptor through p53. *Carcinogenesis*. 2008;29:918–25.
- 435 26. Davis ME. Non-viral gene delivery systems. *Curr Opin Bio-*
436 *technol*. 2002;13:128–31.

Matsubara *et al.*

Induction of Glandular Stomach Cancers in *Helicobacter pylori*-infected Mongolian Gerbils by 1-Nitrosoindole-3-acetonitrile

Satoshi Matsubara^{1,2}, Shinji Takasu¹, Tetsuya Tsukamoto³,
Michihiro Mutoh¹, Shuichi Masuda⁴, Takashi Sugimura¹, Keiji
Wakabayashi^{1,4} and Yukari Totsuka^{1,*}

¹Cancer Prevention Basic Research Project, National Cancer
Center Research Institute, 1-1, Tsukiji 5-chome, Chuo-ku,
Tokyo 104-0045, Japan

²Food Research Department, Yakult Central Institute for
Microbiological Research, 1796, Yaho, Kunitachi-shi, Tokyo
186-8650, Japan

³Department of Pathology and Matrix Biology, Mie University
Graduate School of Medicine, 2-174 Edobashi, Tsu-shi, Mie
514-8507, Japan

⁴Department of Food and Nutritional Sciences, Graduate School
of Nutritional and Environmental Sciences, University of
Shizuoka, 52-1, Yada, Shizuoka 422-8526, Japan

*To whom correspondence should be addressed. Tel:

+81-3-3542-2511;

Fax: +81-3-3543-9305;

Email: ytotsuka@ncc.go.jp

Key words: gastric cancer, *Helicobacter pylori*, Mongolian gerbil, 1-nitrosoindole-3-acetonitrile, indole-3-acetonitrile

Abbreviations: DMSO, dimethyl sulfoxide; *H. pylori*, *Helicobacter pylori*; H&E, hematoxylin and eosin; MG, Mongolian gerbil; MNNG, *N*-methyl-*N'*-nitro-*N*-nitrosoguanidine; MNU, *N*-methyl-*N*-nitrosourea; NIAN, 1-nitrosoindole-3-acetonitrile.

Appropriate category: Carcinogenesis

Matsubara *et al.***Abstract**

Helicobacter pylori (*H. pylori*) infection and high intake of various traditional salt-preserved foods are regarded as risk factors for human gastric cancer. We previously reported that Chinese cabbage contains indole compounds, such as indole-3-acetonitrile, a mutagen precursor. 1-Nitrosoindole-3-acetonitrile (NIAN), formed by the treatment of indole-3-acetonitrile with nitrite under acidic conditions, shows direct-acting mutagenicity. In the present study, NIAN administration by gavage to Mongolian gerbils (MGs) at the dose of 100 mg/kg two times a week resulted in three adduct spots (1.6 adducts/10⁸ nucleotides in total), detected in DNA samples from the glandular stomach by ³²P-postlabelling methods. Treatment with six consecutive doses of 100 mg/kg of NIAN, two times a week for three weeks, induced well- and moderately-differentiated glandular stomach adenocarcinomas in the MGs at the incidence of 31% under *H. pylori* infection at 54 - 104 weeks. Such lesions were not induced in MGs given broth alone, broth + NIAN or infection with *H. pylori* alone. Thus, endogenous carcinogens formed from nitrosation of indole compounds could

be critical risk factors for human gastric cancer development under the influence of *H. pylori* infection.

Introduction

Gastric cancer is the second most frequent cause of cancer death worldwide.¹ Although gastric cancer has become a relatively rare cancer in North America and most Northern and Western European countries, it remains common in East Asia, Eastern Europe, Russia and selected areas of Central and South America.² *Helicobacter pylori* (*H. pylori*) is a well-established major risk factor for gastric cancer,³⁻⁵ and the prevalence of *H. pylori* infection in East Asia countries, including Japan and Korea is reported to be relatively high.^{6, 7} In addition, the risk of gastric cancer is increased with a high intake of various traditional salt-preserved foods.³ In fact, pickled vegetable consumption is reported to increase gastric cancer risk in Japan and Korea.⁸⁻¹⁰ In Korea, kimchi, commonly prepared with Chinese cabbage or radish, is a traditional and popular food, which contains high levels of nitrate (median 1550 mg/kg).¹¹ Furthermore, Chinese cabbage is well known as a pickled

Matsubara *et al.*

vegetable commonly consumed in Japan. Moreover, ingestion of nitrate, mainly from food, is suggested to correlate with mortality from gastric cancer.¹²⁻¹⁴ Ingested nitrate is mainly converted to nitrite by bacteria in the oral cavity after secretion into saliva.¹⁵ Carcinogenic *N*-nitroso compounds can be formed from nitrite and secondary amines under acidic conditions. Furthermore, direct-acting *N*-nitroso compounds, such as *N*-methyl-*N'*-nitro-*N*-nitrosoguanidine (MNNG)¹⁶ and *N*-methyl-*N*-nitrosoourea (MNU),¹⁷ are known to induce cancer in the glandular stomach of experimental animals. Thus, it is suggested that *N*-nitroso compounds that are formed in the stomach under acidic conditions could be positively associated with the risk of gastric cancer. Nitric oxide, formed by nitric oxide synthase, is also reported to contribute to production of *N*-nitroso compounds.¹⁸

We have previously reported that treatments of various foodstuffs with nitrite under acidic conditions produce direct-acting mutagens towards *Salmonella* tester strains.^{19, 20}

Among those foodstuffs, Chinese cabbage is shown to contain three indole compounds, indole-3-acetonitrile,

4-methoxyindole-3-acetonitrile and
4-methoxyindole-3-aldehyde as mutagen precursors.
1-Nitrosoindole-3-acetonitrile (NIAN), an
N-nitroso-substituted compound formed by treatment of
indole-3-acetonitrile with nitrite under acidic conditions, is
a direct-acting mutagen in *S. typhimurium* and Chinese hamster
lung cells,²⁰⁻²² and it is confirmed to form DNA adducts and to
induce DNA single-strand scission in the rat glandular
stomach.^{23, 24} Therefore, NIAN could play some role in gastric
cancer development, as in the case of the well-known
direct-acting mutagens, MNNG and MNU, in animal experiments.^{16,}
^{17, 25}

The Mongolian gerbil (MG) is reported to be susceptible to
colonization by *H. pylori*, and *H. pylori* infection greatly
enhances MNNG or MNU-induced gastric carcinogenesis in MGs.^{26,}
²⁷ Therefore, the MG is considered to be a useful animal model
for evaluating the gastric cancer risk of direct-acting
N-nitroso compounds, with or without *H. pylori* infection.

Chinese cabbage, containing nitrate and indole compounds,
is commonly consumed in East Asian countries, including Japan,

Matsubara *et al.*

Korea and China, in which gastric cancer mortality is very high.

In the present study, DNA adducts were detected with NIAN treatment in the glandular stomach of MGs, and the carcinogenicity of NIAN for gastric cancer *in vivo* was examined.

The results clearly demonstrated that gastric cancer developed with a combination of NIAN administration and *H. pylori* infection in MGs. Possible involvement of indole compounds and nitrate derived from various foodstuffs, including Chinese cabbage, in gastric cancer development in humans is discussed.

Materials and Methods

Materials

Indole-3-acetonitrile was purchased from Tokyo Food Techno Co., Ltd. (Tokyo, Japan), sodium nitrite from Wako Pure Chemical Industries, Ltd. (Osaka, Japan), and ammonium sulfamate from Kanto Chemical Co., Inc. (Tokyo, Japan). Brucella broth was obtained from Becton Dickinson Co. (Cockeysville, MD, USA), and horse serum from Nippon Bio-Supply (Tokyo, Japan).

Preparation of NIAN

The chemical structure of NIAN is shown in Figure 1A. Indole-3-acetonitrile in 27 mM citrate-phosphate buffer (pH 3.0) was treated with 50 mM sodium nitrite for 1 hour at room temperature in the dark, as previously reported.²¹ Nitrosation was stopped by addition of ammonium sulfamate at a final concentration of 50 mM. The reaction solution was filtered and the residue was washed with deionized water, then with n-hexane. The residual paste was dried and stored at -80°C until use. The preparation was >93% pure as judged by its UV absorbance on HPLC.

Bacterial culture

H. pylori (ATCC 43504; American Type Culture Collection, Manassas, VA) was cultured in brucella broth supplemented with 10% heat-inactivated horse serum for 24 hours at 37 °C under microaerobic conditions (5% O₂, 10% CO₂ and 85% N₂), as previously described.²⁸

Animal treatment

Specific pathogen-free male, 6-week-old MGs (MGS/Sea, Kyudo,

Matsubara *et al.*

Fukuoka, Japan) were housed in a biohazard room, air-conditioned at $24\text{ }^{\circ}\text{C} \pm 2\text{ }^{\circ}\text{C}$ and 55% humidity, on a 12 hours light-dark cycle and were allowed free access to commercial diet (CE-2; CLEA Japan Inc., Tokyo, Japan) and water.

In order to analyze the formation of DNA adducts in the glandular stomach of MGs by NIAN treatment, NIAN was dissolved in 50% dimethyl sulfoxide (DMSO), and administered to three MGs by gavage of 0.5 mL solution, two times a week at a level of 100 mg/kg body weight. Two further MGs served as a control group receiving the solvent alone (0.5 mL). At 8 hours after administration of NIAN, both groups of animals were sacrificed under ether anesthesia, and their stomachs were resected and stored at $-80\text{ }^{\circ}\text{C}$ until use. DNA was extracted by a standard procedure with enzymatic digestion of protein and RNA followed by extraction with phenol and chloroform/isoamyl alcohol (24:1, v/v).

The protocol for long-term gastric carcinogenicity in MGs treated with NIAN + *H. pylori* infection is illustrated in Figure 1B. The animals were randomly divided into four groups (groups A-D). Groups A and C were given 50% DMSO without NIAN (0.5 mL),

while groups B and D were orally administrated NIAN (0.5 mL, 100 mg/kg body weight) dissolved in 50% DMSO by gavage, two times a week for three weeks. At 1 week after the last administration, the animals of groups C and D were given an intragastric inoculation of *H. pylori* broth culture (0.5 mL, 0.9×10^8 CFU/animal), while animals of groups A and B were given sterilized broth alone (0.5 mL).²⁸

During the experiments, animals which became moribund or emaciated (<80 g body weight) were sacrificed. At 104 weeks after *H. pylori* infection, all surviving animals were sacrificed under ether anesthesia. At performance of necropsy, all tissues were carefully checked macroscopically and the stomachs and major organs were removed and assessed for macroscopic lesion development. Effective numbers of animals were defined as those surviving until week 54 of the study, when gastric tumors were observed for the first time. In addition, in the *H. pylori*-infected groups, the animals developing gastritis observed on histological examination were regarded as effective. The percentages of gastritis-bearing animals by the single inoculation of *H. pylori* were 62% for group C and